Coastal Engineering 67 (2012) 14–28

Contents lists available at SciVerse ScienceDirect

Coastal Engineering

journal homepage: www.elsevier.com/locate/coastaleng

Modelling morphodynamic response of a tidal basin to an anthropogenic effect: Ley Bay, East Frisian Wadden Sea – applying tidal forcing only and different sediment fractions

D.M.P.K. Dissanayake [a,*], A. Wurpts [a,1], M. Miani [a,2], H. Knaack [a,3], H.D. Niemeyer [a,4,5], J.A. Roelvink [b,c,6]

[a] Coastal Research Station, Lower Saxony Water Management, Coastal Defence and Nature Conservation Agency, An der Mühle 5, D-26548, Norderney, Germany
[b] UNESCO-IHE Institute for Water Education, PO Box 3015, 2601 DA, Delft, The Netherlands
[c] Technical University of Delft, PO Box 5048, 2600 GA, Delft, The Netherlands Deltares, PO Box 177, 2600 MH, Delft, The Netherlands

ARTICLE INFO

Article history:
Received 27 September 2011
Received in revised form 1 April 2012
Accepted 3 April 2012
Available online xxxx

Keywords:
Anthropogenic effect
Ley Bay
Leyhörn peninsula
Sediment fractions
Morphological evolution
Delft3D
East Frisian Wadden Sea

ABSTRACT

Morphodynamic response to an anthropogenic effect (construction of a peninsula) is investigated using the state-of-the-art Delft3D numerical model based on the Ley Bay area in the East Frisian Wadden Sea. Model simulations span a duration of 15 years applying tidal boundary forcing only and two bed sediment compositions; single (d_{50} = 0.2 mm)- and multiple (mud, fine-sand (0.25 mm) and coarse-sand (0.60 mm))-fractions. Finally, the effect of the initial distribution of sediment fractions is investigated.

Application of the multiple sediment fractions resulted in strong sediment import into the Ley Bay in contrast with the case for a single sediment fraction. Temporal and spatial evolution of larger-scale basin elements (e.g. channels, tidal flats) indicate that the impact of the peninsula is better predicted using the multiple sediment approach. Agreement between the predicted morphology and the data is fair in deep water areas (> 3 m) compared to the shallow water areas (< 2 m) in the bay. These predictions are further improved after application of an initially distributed bed sediment composition. Therefore, the optimal prediction of the anthropogenic effect is obtained under the latter case implying the requirement of applying a stable bed sediment composition in line with the imposed boundary forcings.

On-going work focuses on more detailed bed configuration around the peninsula (e.g. including possible dredging and dumping effects) and the wave boundary forcing.

1. Introduction

Human interference (i.e. anthropogenic effects) namely diking, land reclamation, peat-cutting and damming of channels since the Middle Ages has had a great influence on the present-day morphology of the Wadden Sea tidal basin systems. Further, reinforcing of existing dunes to serve as dikes, construction of jetties and closing of tidal basins (e.g. Zuider Sea (Thijsse, 1972; Elias et al., 2003)) had major impacts on the Wadden Sea evolution. Eastern part of the Wadden Sea (i.e. East Frisian Wadden Sea) showed drastic changes of bed evolution due to anthropogenic effects. Numerous examples are found on the Lower Saxony coast, e.g. Ley Bay, Harle Bay, Jade Bay etc. (Homeier et al., 2010). Present analysis focuses on the bed evolution of Ley Bay due to construction of a peninsula '*Leyhörn*'.

The Leyhörn peninsula has been constructed in 1984 to enable a number of functions, i.e. coastal safety, navigational access and inland drainage. Level of efficiency of these functions is directly related to the morphological set-up of the Ley Bay area. In turn, strong morphological changes are expected due to disturbance the Leyhörn peninsula is causing to the existing system. Therefore, a better insight of the possible bed changes of the bay is required to allow effective and efficient planning and management strategies. The overarching aim of this study is to establish a morphological model which can hindcast the bed evolution due to the effect of Leyhörn. Such a model provides more insight into the dominant physical processes of the Ley Bay morphology. The study period extends for 15 years from 1975 to 1990 and thus it is necessary to adopt a modelling technique of long-term (i.e. decadal) bed evolution.

Long-term bed evolution of tidal basin systems is investigated applying empirical and numerical models. Empirical approaches make use of historical data to interpret the bed evolution of the inlet/basin systems (Elias, 2006; Homeier et al., 2010; Knaack and Niemeyer, 2001). Homeier et al. (2010) used the historical topography charts of

* Corresponding author. Tel.: +49 49 32 916 147; fax: +49 49 32 1394.
E-mail addresses: Pushpa.Dissanayake@nlwkn-ny.niedersachsen.de (D.M.P.K. Dissanayake), andreas.wurpts@nlwkn-ny.niedersachsen.de (A. Wurpts), marco.miani@nlwkn-ny.niedersachsen.de (M. Miani), Heiko.Knaack@nlwkn-ny.niedersachsen.de (H. Knaack), Niemeyer.crs@t-online.de (H.D. Niemeyer), d.roelvink@unesco-ihe.org (J.A. Roelvink).
[1] Tel.: +49 49 32 916 121; fax: +49 49 32 1394.
[2] Tel.: +49 49 32 916 100; fax: +49 49 32 1394.
[3] Tel.: +49 49 32 916 150; fax: +49 49 32 1394.
[4] Presently retired.
[5] Tel.: +49 49 32 916 141; fax: +49 49 32 1394.

0378-3839/$ – see front matter © 2012 Elsevier B.V. All rights reserved.
doi:10.1016/j.coastaleng.2012.04.001

the East Frisian tidal basins from 1650 to 1960 to describe the human interference and self adaptation of these systems with respect to the long-term bed evolution. Elias (2006) analysed the historical development of the Texel inlet/basin system due to the effect of *Afsluitdijk* (i.e. Closure dike). Knaack and Niemeyer (2001) discussed the bed evolution of the Ley Bay area from 1960 to 1999 indicating the impact of the Leyhörn peninsula. However, these approaches depend on the data availability (i.e. historical data are very sparse) and thus it is difficult to investigate the formation and migration of the bed features and the underlying processes. In contrast, the numerical approaches can be adopted to investigate bed evolution with high spatial and temporal resolution and thereby provides more insight of the dominant processes. The state-of-the-art Delft3D model is nowadays increasingly applied to investigate long-term (i.e. several decades) bed evolution in estuarine and coastal systems (e.g. Dastgheib et al., 2008; Dissanayake et al., 2009; Van der Wegen, 2010). Further, these studies have shown that the tide dominated coastal systems can to a reasonable extent be modelled imposing the tidal boundary forcing only. Therefore, the present study also employs the Delft3D model with tidal boundaries only to hindcast the bed evolution of the Ley Bay from 1975 to 1990, with due to the impact of the Leyhörn peninsula.

2. Study area

Ley Bay is a part of the Oster-Ems basin which is located between Borkum (west) and Juist (east) barrier islands in the East Frisian Wadden Sea (Fig. 1). Average tidal range of the Oster-Ems inlet is about 2.8 m and yearly mean wave height seaward from the inlet is about 1 m. This inlet/basin system can be classified as a mixed-energy tide dominated environment (Hayes, 1979). Therefore, the tidal forcing is the dominating factor shaping the hydrodynamics and in turn morphodynamics of the study area. Ley Bay is characterised by a hierarchy of tidal gullies and tributaries of the tidal inlet (Leysander Priel, Greetsieler Wattfahrwasser and Norder Außentief, see Fig. 1). A large part of the basin area consists of intertidal flats and extended supratidal salt marshes with unique fauna and flora. Human intervention in this area was required in order to mitigate coastal zone management problems, i.e. safety against storms, navigational access of fishing vessels to Greetsiel harbour, maintaining inland drainage.

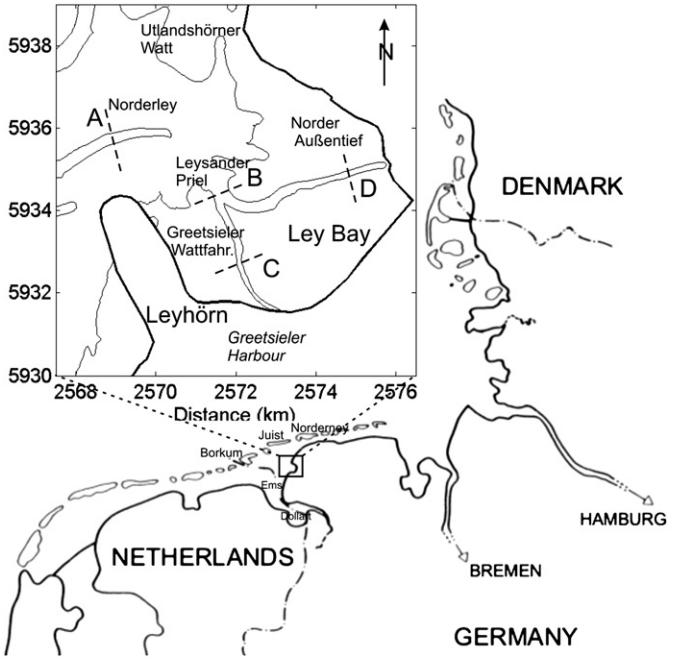

Fig. 1. Location of the Ley Bay area in the East Frisian Wadden Sea and channel cross-sections A, B, C and D (see Fig. 17).

The catastrophic storm surges of the 14th century widened and extended the Ley Bay area. The flooded areas were highly vulnerable to erosion during storm surges, because the subsurface consisted of peat layers. After such events, the balance between tidal forcing and morphology was disturbed and strong sedimentation occurred to re-establish the dynamic equilibrium (Niemeyer, 1991). Then, salt marshes were developed at the borders of the bay which in turn enhanced the bay sedimentation together with the associated land reclamation work (Homeier, 1969). Growth of salt marshes allowed subsequent reclamation and diking of formerly lost areas. In recent years, diking of intertidal flats rather than supratidal salt marsh areas has been implemented, which has a much higher impact on hydrodynamical-morphological interactions (Niemeyer, 1991). These measures ultimately resulted in accelerated sedimentation at the borders of the bay and in the access channel affecting to the inland drainage and the navigational access respectively. Therefore, the inland drainage had to be enhanced by of pumping while the navigational requirements were achieved by the maintenance dredging spending millions of Euros annually.

Several strategies were formulated in order to address these coastal management issues, of which the plan for enclosing of the Ley Bay area became more urgent because the existing dikes could not meet the safety requirements (Niemeyer, 1984). However, this option resulted in a controversial public discussion with respect to the economic and ecological implications (Hartung, 1983). Therefore, the State Government of Lower Saxony demanded another solution based on the newly established social priorities and the traditional coastal zone management strategies in the Wadden Sea area. As an alternative, the Leyhörn peninsula was constructed in 1984 to enable the following functionalities (Niemeyer, 1994),

- Safety of the coastal area against storm surges.
- Conservation of the Ley Bay as an unique ecological area.
- Re-establishment of inland drainage mainly by free-flow due to hydraulic gradient.
- Navigational access without maintenance dredging.
- Conservation of the traditional functions of the adjacent fishing harbour (i.e. Greetsiel, see Fig. 1).

3. Approach

3.1. Numerical modelling

Present study extensively uses the process-based model Delft3D developed by Deltares (formerly WL | Delft Hydraulics). The model allows one- (1D), two- (2DV and 2DH) and three-dimensional (3D) simulations. It also allows the discretisation of the study area in rectilinear, curvilinear or spherical co-ordinate systems. The primary variables of flow, water level and velocity, are specified on Arakawa C staggered grids. The model structure is shown in Fig. 2. As 3D processes such as vertical density stratification are not of critical importance to reach the objectives of the present study, here a 2DH version (depth averaged area model) of Delft3D is employed. Furthermore, previous studies (Dissanayake et al., 2012; Dissanayake et al., 2009; Van der Wegen et al, 2008; Van der Wegen and Roelvink, 2008; Dastgheib et al., 2008) have shown that application of the 2DH version is able to develop major channel/shoal pattern of the tidal basins in the Wadden Sea as present in the measured data.

3.1.1. Hydrodynamics

The unsteady shallow water equations are solved via the Alternating Direction Implicit (ADI) method to compute the hydrodynamics (Leendertse, 1987; Stelling, 1984; Stelling and Leendertse, 1991). The system of equations consists of the horizontal momentum equations, the continuity equation, the transport equation and a turbulence closure model. The application of these equations in Delft3D is described in detail by Lesser et al. (2004) and is hence not reproduced here.

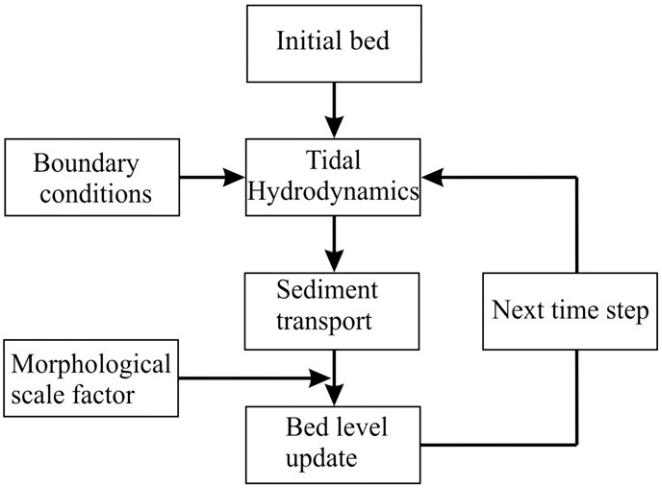

Fig. 2. Schematised diagram of FLOW online-morphological model in Delft3D.

3.1.2. Sediment transport

Sediment transport is separately estimated for non-cohesive and cohesive sediment fractions. Non-cohesive transport (>0.063 mm) uses the Van Rijn (1993) formulas based on the depth-integrated advection–diffusion equation while cohesive transport (≤0.063 mm) uses the Partheniades' erosion and Krone's deposition formulas (Partheniades, 1965).

3.1.2.1. Non-cohesive sediment transport. In Van Rijn's (1993) formulations, the sediment transport below and above the reference height '*a*' is defined as bed load and suspended load respectively. The reference height is mainly a function of water depth and a user defined reference factor. Sediment entrainment into the water column is facilitated by imposing a reference concentration at the reference height.

Suspended sediment transport is estimated based on the advection–diffusion equation. In depth-averaged simulations, the 3D advection–diffusion equation is approximated by the depth-integrated advection–diffusion equation:

$$\frac{\partial h\bar{c}}{\partial t}+\bar{u}\frac{\partial h\bar{c}}{\partial x}+\bar{v}\frac{\partial h\bar{c}}{\partial y}-D_H\frac{\partial^2 h\bar{c}}{\partial x^2}-D_H\frac{\partial^2 h\bar{c}}{\partial y^2}=h\frac{\bar{c}_{eq}-\bar{c}}{T_s} \tag{1}$$

where; D_H, the horizontal dispersion coefficient (m^2/s); $\bar{c}$, the depth averaged sediment concentration (kg/m^3); $\bar{c}_{eq}$, the depth-averaged equilibrium concentration (kg/m^3) as described by Van Rijn (1993) and T_s is an adaptation time-scale (s). T_s is given by (Galappatti,1983),

$$T_s=\frac{h}{w}T_{sd} \tag{2}$$

where, h is the water depth, w is the sediment fall velocity and T_{sd} is an analytical function of shear velocity u_* and w. Where, u_* is given by:

$$u'_{*,c}=\left(0.125f'_c\right)^{0.5}\bar{u} \tag{3}$$

Bed load sediment transport is given by:

$$|S_b|=f_{bed}\eta\times 0.5\rho_s d_{50}u'_*D_*^{-0.3}T_a \tag{4}$$

where, D_* is non-dimensional particle diameter.

$$D_*=d_{50}\left[\frac{(s-1)g}{\upsilon^2}\right]^{1/3} \tag{5}$$

and, T_a is the non-dimensional bed shear stress.

$$T_a=\frac{\left(\tau'_b-\tau_{b,cr}\right)}{\tau_{b,cr}} \tag{6}$$

For Equations 1–6, S_b, is bed load transport rate (kg/m/s); f_{bed} is a calibration factor (−); η is relative availability of sand at bottom (−); d_{50} is the mean grain diameter (m); ρ_s is density of sediment (kg/m3); f'_c is current-related friction factor (−); $\bar{u}$ is the depth average velocity (m/s); s is relative sediment density (−); υ is the horizontal eddy viscosity (m^2/s); and, $\tau_{b,cr}$ is critical bed shear stress for initiation of sediment transport (N/m^2).

3.1.2.2. Cohesive sediment transport. The cohesive transport is modelled applying the Patheniades-Krone formulations (Partheniades, 1965). Erosive (E) and deposition (D) fluxes read as,

$$E=MS_e\left(\tau_{cw},\tau_{cr,e}\right)^e \tag{7}$$

$$D=w_s c_b S_d\left(\tau_{cw},\tau_{cr,d}\right) \tag{8}$$

and

$$\begin{aligned}S_e\left(\tau_{cw},\tau_{cr,e}\right)&=\left(\frac{\tau_{cw}}{\tau_{cr,e}}-1\right)for\,\tau_{cw}>\tau_{cr,e}\\&=0\qquad for\,\tau_{cw}\le\tau_{cr,e}\end{aligned} \tag{9}$$

$$\begin{aligned}S_d\left(\tau_{cw},\tau_{cr,d}\right)&=\left(\frac{\tau_{cw}}{\tau_{cr,d}}-1\right)for\,\tau_{cw}>\tau_{cr,d}\\&=0\qquad for\,\tau_{cw}\ge\tau_{cr,d}\end{aligned} \tag{10}$$

where; E ($kg/m^2/s$); D ($kg/m^2/s$); M, erosion parameter ($kg/m^2/s$); w_s, sediment fall velocity (m/s); c_b, near bottom concentration (kg/m^3); τ_{cw}, maximum shear stress due to waves and currents (N/m^2); $\tau_{cr,e}$, critical shear stress for erosion (N/m^2); $\tau_{cr,d}$, critical shear stress for deposition (N/m^2).

3.1.3. Morphodynamics

Coastal morphodynamic changes occur at time scales that are about 1 to 2 orders of magnitude greater than the hydrodynamic time scales (Stive et al., 1990). Therefore, in a conventional morphodynamic model, many hydrodynamic computations need to be performed to achieve significant morphological changes. Thus, conventional morphodynamic simulations, by necessity have been very long and inefficient. However, the morphological scale factor (*MORFAC*) approach presented by Roelvink (2006) and Lesser et al. (2004), which is used in Delft3D for bed level updates, circumnavigates this problem. In this approach, which is particularly geared at significantly improving the efficiency of morphodynamic calculations, the bed level changes calculated at each hydrodynamic time step are scaled up by multiplying erosion and deposition fluxes by a constant (*MORFAC*).

$$\Delta t_{morpho\,logy}=MORFAC\times\Delta t_{hydrodynamic} \tag{11}$$

This approach also allows accelerated bed level changes to be dynamically coupled (on-line) with hydrodynamic computations (see Fig. 2). Therefore, long-term morphological changes can be simulated at reasonable computational cost. In general usage, several trial simulations are undertaken with incremental *MORFAC*s to determine the highest *MORFAC* value that can be used safely for a given simulation (see section 3.2.4). Delft3D also recommends that bed level changes within one tidal cycle should not exceed 10% of the local water depth.

3.2. Model implementation

3.2.1. Bathymetry and grid set-up

Fig. 3 shows the measured bathymetries (i.e. 1975 and 1990) of the Oster-Ems basin. The model area covers the entire Oster-Ems basin. The1975 bed is taken as the initial model bed. The enclosed rectangle in Fig. 3b (1990 bed) indicates the Ley Bay area and the Leyhörn peninsula (see, outline of the peninsula on the 1975 bed (Fig. 3a). Averaged depth of the Ley Bay area (on 1975 bed) is about +0.5 m MSL implying that tidal flats and salt marshes enclose a large part of the bay area. On the 1975 bathymetry, there is a well-pronounced channel system in the Ley Bay area (see number 2, 3 and 4 in Fig. 3a). Leysander Priel (2 in Fig. 3a) is branched into two channels, namely Greetsieler Wattfahrwasser (3 in Fig. 3a) and Norder Außentief (4 in Fig. 3a). The Greetsieler channel provided the navigational access to the Greetsieler harbour while the Norder channel was mainly used to allow inland drainage by pumping. On the 1990 bathymetry, the Leyhörn peninsula (length ~ 3.5 km and width ~ 1.5 km) is shown whereas the access channel is not yet found because it has been implemented in 1991 (Knaack and Niemeyer, 2001). The Ley Bay area shows strong sedimentation, which results in the disappearance of the Greetsieler and Norder channels (Fig. 3b). However, Leysander Priel appears to be strong in comparison to the 1975 bathymetry. This is an indication of strong current pattern at the entrance of the bay due to the presence of the peninsula.

Fig. 3c shows the model grid enclosing the Oster-Ems basin. Averaged grid size is about 200 m × 200 m. However, the Ley Bay area (~5.0 km × 5.0 km) has a high resolution (20 m × 20 m) in order to represent the bay channel pattern.

3.2.2. Boundary forcing

The Oster-Ems basin has a mixed energy tide dominated inlet (Sha, 1989). Morphodynamics of this area is mainly governed by tidal forcings (Ridderinkhof, 1988; Wang et al., 1995). Model approaches applying the tidal boundary forcing only were able to reproduce typical morphological patterns in the Wadden Sea tidal basins (Dissanayake et al., 2009, 2012; Van der Wegen and Roelvink, 2008; Dastgheib et al., 2008). Therefore, present analysis also employs the tidal boundary forcing only.

Tidal forcing of the Oster-Ems model is based on a Continental shelf model which has been well calibrated and enclosed entire North Sea area (Verboom et al., 1992). These boundary forcings were estimated via a nested modelling approach in order to transfer the offshore (North Sea) hydrodynamic characteristics up to the Oster-Ems model boundaries (Wadden Sea). Model nesting was applied under two phases, 1) Continental shelf model to Coastal model, 2) Coastal model to Oster-Ems model. Initially, the continental shelf model was simulated for 3 months from June to September in 1975 based on the astronomical boundary conditions and then the water level elevations were extracted at the boundaries of the coastal model. Subsequently, the coastal model (see Knaack et al., 2003) was simulated using the extracted water levels to get the boundary forcings of the Oster-Ems model which has three open boundaries viz. north, east and west. The north boundary is located at the inlet gorge and the east and west boundaries are in the Wadden Sea side opposite to the Norderney tidal basin and the Ems estuary respectively (see Fig. 1). Preliminary results showed that applying three water level boundaries of the Oster-Ems model (at north, east and west), developed unrealistic velocity patterns. Therefore, flow velocity is applied for the northern boundary while the lateral two boundaries (i.e. east and west) use water levels. Such combination of boundary forcings increases the numerical stability (refer Delft3D FLOW user manual). It is emphasised that other boundary forcings such as waves and storm effects have been excluded in the present analysis.

3.2.3. Bed sediment composition

This analysis mainly used two bed sediment compositions to investigate the long-term evolution of the Ley Bay area, 1) Single sediment fraction and 2) Multiple sediment fractions.

Average sediment size of the Wadden Sea basins is about 0.2 mm. Therefore, long-term modelling approaches use a single sediment fraction of 0.2 mm (d_{50}) to investigate bed evolutions (see Dastgheib et al., 2008; Dissanayake et al., 2009, 2012). These studies have shown that application of the single sediment fraction potentially develops the typical channel/shoal patterns of tidal basins. Thus, present study also adopts this sediment fraction as one option of the bed compositions. However, it is emphasised that application of a single sediment fraction is a highly simplified version of the nature (Van der Wegen, 2010). Application of the multiple fractions includes three sediment fractions viz. mud (≤ 0.063 mm), fine-sand (0.25 mm) and coarse-sand (0.60 mm) based on the study of Herrling and Niemeyer (2008). They have reconstructed spatial sediment thickness of the Dollard-Ems estuary area (i.e. adjacent estuary on the west of the Oster-Ems basin, see Fig. 1) using the Rijkswaterstaat Sediment Atlas (2007). Their model domain encloses the area of the Oster-Ems basin also and that allows using this sediment information for the present analysis. Three sediment fractions were allocated with vertical and horizontal discretisations. In vertically, the bed strategraphy consists of 10 layers each having 1 m thick, of which the first two layers have a spatially varying mixture of only mud and fine-sand. Spatial discretisation of these two fractions is based on Herrling and Niemeyer (2008). From third layer onwards, there is a uniform mixture of fine-sand and coarse-sand (i.e. 50% of each fraction based on sediment mass). Fig. 4 shows the sediment distribution at the top layer of the 1975 bed (note: outline indicates the peninsula). Mud fraction is concentrated along the shoreline of the bay. Fine-sand spreads over the entire basin while coarse-sand is not found at the top layer.

Bed composition with multiple fractions was implemented in the Delft3D model using a layered bed stratigraphy (refer Delft3D FLOW

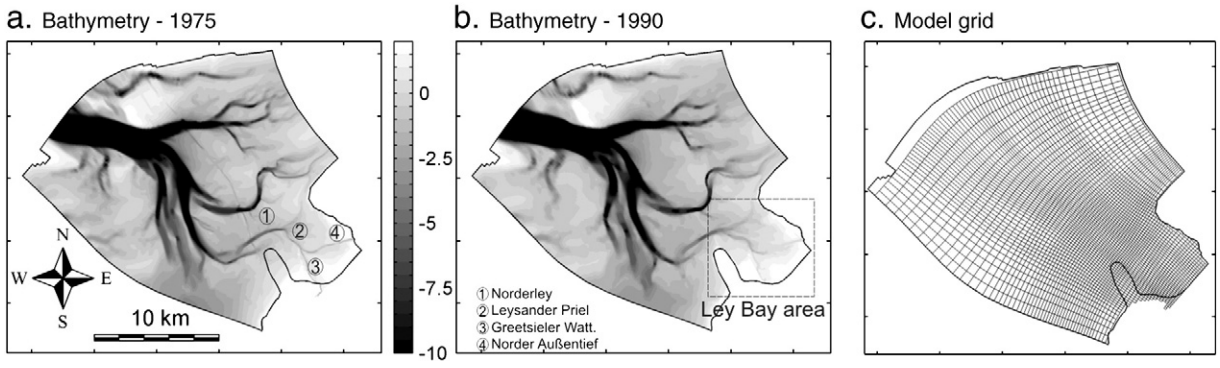

Fig. 3. Measured bathymetries of the model area (Oster-Ems basin), 1975 bed with the layout of Leyhörn (a), 1990 bed with Ley Bay analysis area (b) and Model grid (every 5th grid line shown) (c).

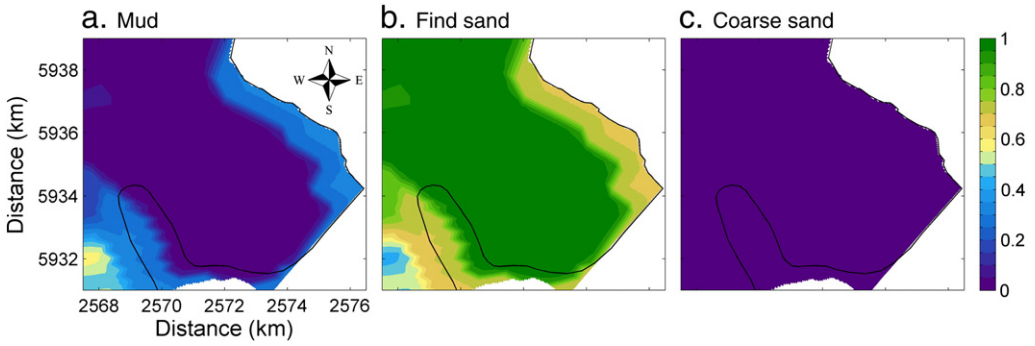

Fig. 4. Distribution of sediment fractions of the top layer in multiple sediment approach, a) Mud, b) Fine-sand and c) Coarse-sand.

user manual). The top most layer is divided into the transport layer (0.4 m following Van der Wegen, 2010) and the first under layer after the first time step according to the user defined thickness heights. During erosion, sediment is lost from the transport layer, which is recharged by the first under layer. After the sediment content of the first under layer is empty, the same process repeats with the second under layer and so on. During sedimentation, the transport layer receives sediment and passes into a newly created under layer beneath. After the new layer is saturated (i.e. 1 m thickness), another under layer is formed and the same process continues up to the user defined number of under layers (i.e. 10). The bed topography changes by shrinking of the under layers in case of the erosion while expanding them in the sedimentation process.

Applying the multiple bed composition, erosion of sand fractions from the sediment bed and in turn the transport capacity depends on the mud content at the bed surface. Fine particles easily escape to the water column compared to the coarse particles. Deposition of sediment is assumed to be independent for sand and mud. Erosion of mud is determined by the user defined erosion parameter (see *Eq.* 9). Sensitivity of bed erosion in the Ley Bay to this parameter is discussed in section 4.2.

At the open boundaries, no sediment concentration is prescribed for mud and sand fractions whereas suspended sediment, advected by tidal movement, is present. This means that sediment will leave the model domain and ideally come back after turning of the tide at the boundaries. This process is implemented in the model in terms of a Thatcher-Harleman time lag that stores sediment concentrations and reintroduces these at the boundary when the tide returns (see Delft3D FLOW manual).

3.2.4. Selection of MORFAC

As discussed in section 3.1.3, the long-term morphological changes are simulated in terms of *MORFAC*. At present, there is no priori determination of the highest *MORFAC* value for a specific study area. Therefore, a sensitivity analysis was undertaken applying three *MORFAC*s (30, 60 and 120) to determine the optimal value that can be safely applied in this analysis. Hydrodynamic period of these simulations are about 6 months, 3 months and 1.5 months respectively and hydrodynamic time step is 1 minute following the previous modelling of the study area (see Knaack et al., 2003).

For the sake of simplicity, the peninsula was implemented on the initial bathymetry without including the dike and the models were simulated applying tidal boundary and the single bed sediment composition (see section 3.2.2 and 3.2.3). Predicted bed evolutions are compared together and with the 1990 data to investigate the relative influence of *MORFAC*.

3.2.4.1. Bed evolution. Fig. 5 shows the predicted 1990 beds under three *MORFAC* approaches with the measured data. In contrast to the data, predicted morphologies have two pronounced channels in the Ley Bay and they appear to be similar in all cases. Therefore, visual discern among the three model predictions is difficult.

Quantitative analysis of the bed evolutions was carried out in order to compare and contrast the effect of *MORFAC*.

3.2.4.2. Erosion and Sedimentation. Erosion and sedimentation of the Ley Bay excluding the peninsula area was estimated for the three *MORFAC* approaches (Fig. 6). In all cases, sedimentation is about 0.55 Mm^3, erosion is about 0.90 Mm^3 while the net change is about -0.35 Mm^3 (see Fig. 6a, b and c). However, the results show that both *MORFAC* = 30 and *MORFAC* = 60 tend to show similar variation in sedimentation, erosion and net change while *MORFAC* = 120 is different. Therefore, the first two *MORFAC*s (30 and 60) appear to have similar effects on bed level changes while the third is different.

3.2.4.3. Model skill. Model skill under the three *MORFAC* approaches was further analysed in terms of Brier Skill Score (BSS) (Sutherland et al., 2004). It is noted that the *BSS* is not a perfect method to evaluate model performance especially where individual characteristics such as basin infilling, lateral displacement and rate of bifurcation of channels etc. are concerned. However, at this point in time, this is the most widely adopted method to objectively assess the model skill (Pedrozo-Acuna et al., 2006; Roelvink et al., 2009; Ruessink et

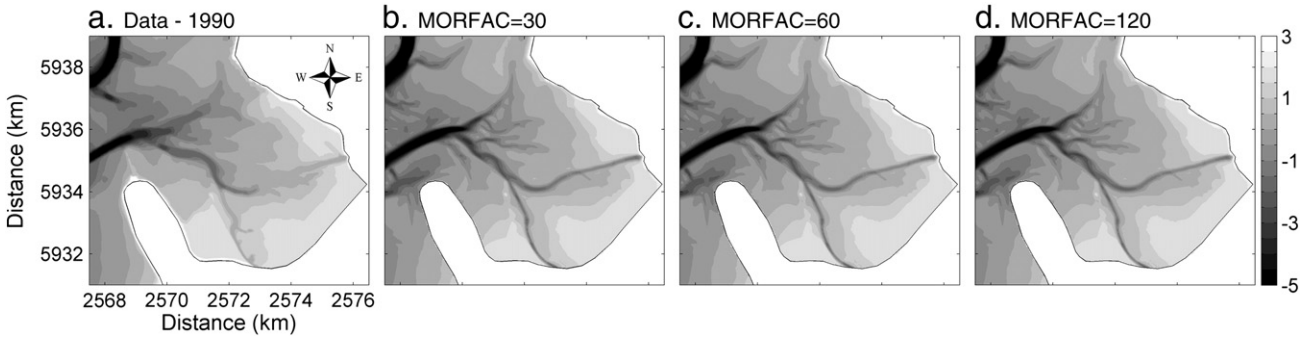

Fig. 5. Comparison of measured data (a) and predicted bathymetries under different MORFAC value; 30 (b), 60 (c) and 120 (d).

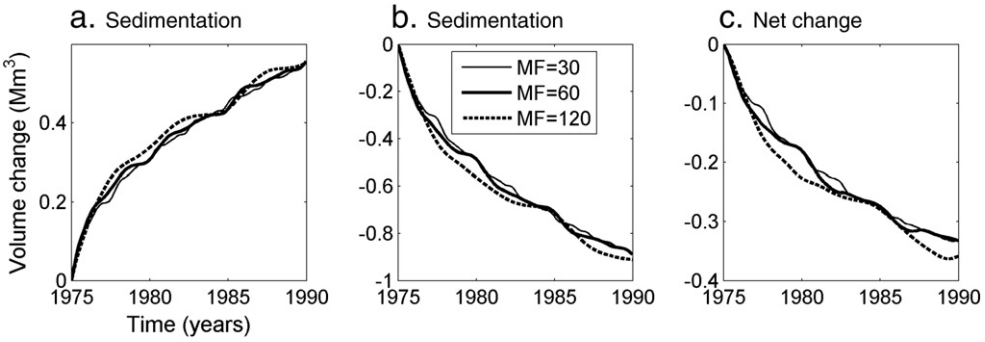

Fig. 6. Sedimentation and erosion in the Ley Bay in three *MORFAC* approaches.

al., 2003; Ruggiero et al., 2009), and due to the lack of a better alternative, the *BSS* approach is adopted to evaluate the model skill. The *BSS* is defined by Sutherland et al. (2004) as,

$$BSS = \frac{\alpha - \beta - \gamma + \varepsilon}{1 + \varepsilon} \tag{9}$$

where, $\alpha = r^2_{Y'X'}$ $\beta = \left(r_{Y'X'} - \frac{\sigma_{Y'}}{\sigma_{X'}}\right)^2$ $\gamma = \left(\frac{\langle Y'\rangle - \langle X'\rangle}{\sigma_{X'}}\right)^2$ $\varepsilon = \left(\frac{\langle X'\rangle}{\sigma_{X'}}\right)^2$ and $X' = z_{1990} - z_{1975}$, $Y' = z_{\mathrm{mod\ }el} - z_{1975}z$, bed levels in 1975 ($z_{1975}$), 1990 ($z_{1990}$) and model beds with *MORFAC* = 30, 60 and 120 (z_{model})

- α a measure of bed form phase error and perfect model gives $\alpha = 1$
- β a measure of bed form amplitude error and perfect model gives $\beta = 0$
- γ an average bed level error and perfect model gives $\gamma = 0$
- ε a normalization term which indicates the measurement error

In the above definition of the *BSS*, a value of 1 indicates an excellent comparison between the measurements and the model results. Negative *BSS* values imply large differences between the modelled and measured bathymetries.

Sutherland et al. (2004) give the following classifications for the assessment of model performance against the *BSS* (Table 1).

Fig. 7 shows the estimated variations from 1975 to 1990 of Phase, Amplitude, Mean value and *BSS* as defined by Sutherland et al. (2004). Results indicate similar trend in all cases. Final values of the 1990 predicted bed are away from the values of a perfect model prediction. This is partly due to implementing the peninsula on the initial model bed. However, these values imply the relative effect of the *MORFAC* approaches. It is still apparent that both *MORFAC* = 30 and *MORFAC* = 60 cases show similar pattern while the other seems to have a different variation. This is noticeable in Mean value.

Table 2 shows estimated values of the 1990 predicted beds. Maximum difference among the three approaches with respect to the *MORFAC* = 30 case is about 4%, 5% and 8% for Phase, Amplitude and Mean value respectively. Therefore, the mean value appears to have a significant influence of the *BSS* value. The *MORFAC* = 60 case results in the highest *BSS*.

This analysis suggests that the effect of *MORFAC* is marginal as far as the overall bed level change is concerned. Both *MORFAC* = 30 and *MORFAC* = 60 cases showed more or less similar evolution from 1975 to 1990 and the optimal *BSS* of the 1990 predicted bed was obtained under the *MORFAC* = 60 case. Therefore, *MORFAC* = 60 was employed to investigate the Ley Bay evolution under different scenarios (see section 3.2.5).

Table 1
Classification for Brier Skill Score by Sutherland et al. (2004).

Classification	BSSSutherland
Excellent	1.0 – 0.5
Good	0.5 – 0.2
Reasonable/Fair	0.2 – 0.1
Poor	0.1 – 0.0
Bad	<0.0

3.2.5. Model simulations

Initially, the hydrodynamic simulations were undertaken to compare the predicted and the measured water levels in the Ley Bay based on the 1975 bed. Then, a sensitivity analysis was carried out to optimise the model parameters related to the cohesive sediment transport.

The morphological simulations span a period of 15 years from 1975 to 1990 in two stages, 1) No peninsula stage and 2) Peninsula stage. The no peninsula stage extends from 1975 to 1984 considering the fact that the peninsula has been constructed in 1984. The predicted 1984 bed is subsequently used to simulate the peninsula stage from 1984 to 1990 (i.e. applying the peninsula on the 1984 predicted bed). The long-term bed evolution is obtained applying the *MORFAC* technique (*MORFAC* = 60, see section 3.2.4).

Table 3 shows the morphological simulations (M1 and M2) which differ due to having different initial sediment characteristics. M1 uses the single sediment fraction while M2 is simulated applying multiple sediment fractions (see section 3.2.3). It is noted that all these models use spatially varying bed roughness (i.e. Manning's value) which changes with the water depth as discussed in Hartsuiker (2003).

It is emphasised that these models (see Table 3) are simulated without including dredging and dumping works which have been undertaken, prior to the peninsula construction for maintenance of the navigational channel to the Greetsiel harbour, Greetsieler Wattfahrwasser (see Fig. 1, this was initially created by dredging in 1973 (Niemeyer, 1991, and during the peninsula construction. These activities are expected to have an impact on the Ley Bay morphology.

Our focus is to develop a morphological model which can describe the effect of the Leyhörn peninsula on the Ley Bay morphology. Therefore, the bed evolution is analysed based on the Ley Bay area only (see Fig. 3b).

4. Results and Discussion

4.1. Hydrodynamics

4.1.1. Comparison with measured water level data

In 1975, only monthly averaged water level data are available at the tidal station, Norderney Riffgat (~ 5.0 m depth) which is located on the adjacent tidal basin to the east of the model area (see Fig. 1). Therefore, these water levels are used to get some insight of the model predicted water levels. Such comparison provides qualitative impression of the model behaviour. Initially, the measured water levels at Norderney Riffgat were transferred to the Ley Bay area (i.e. Greetsieler Nackenlegde, GN (~ 1.5 m depth), see Fig. 3a) applying a

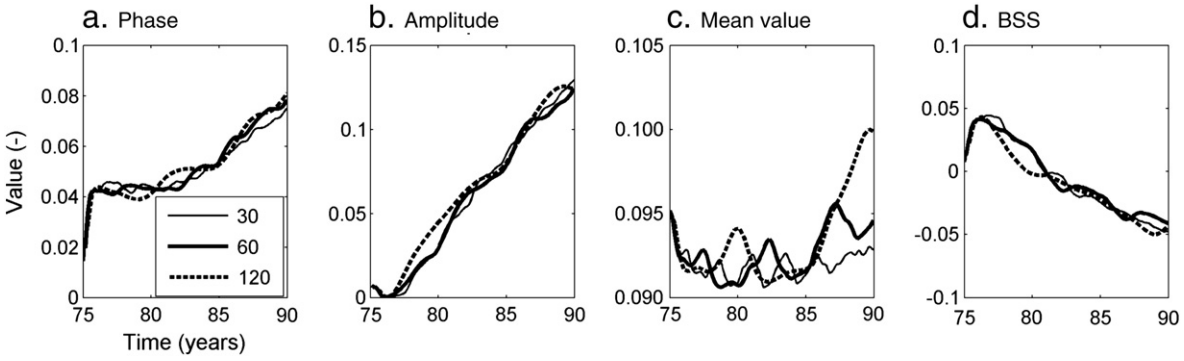

Fig. 7. Comparison of Phase (a), Amplitude (b), Mean value (c) and BSS (d) under three MORFAC approaches according to the definition of Sutherland et al. (2004).

linear relation as proposed by Niemeyer et al. (2001). Then, the model predicted water levels were monthly averaged and that resulted in three LW (Low Water) and HW (High Water) points due to the three-month of hydrodynamic period of the simulation (Fig. 8).

Fig. 8 shows water levels at Norderney Riffgat (blue-dash-line), transferred to GN (red-line) and model predicted at GN (black-circle). Measured data indicate that the tidal range increases while propagating the tidal wave into the shallow area and the difference in LW is higher than that of HW. This is typically found in the Wadden Sea basins (Knaack et al., 2003). Predicted water levels at GN show away from that of the data, whereas the tidal range appears to correspond in both cases. Further, both data and predicted water levels comparatively agree during HW rather than LW. These differences are embedded with a number of reasons. Firstly, the data show lower LW level implying a higher depth at GN in comparison to the model bed. This is probably due to applied grid resolution (i.e. grid sizes 20 m × 20 m). Furthermore, it is generally accepted that the models weakly represent LW in the Wadden Sea area due to the extensive tidal flats which are not properly encountered of the measured bed (see Dissanayake et al., 2009). Secondly, the model used the same bathymetry during the three-month period whereas the topography in nature tends to change due to the strong sedimentation (Knaack and Niemeyer, 2001). This is evident having similar model predictions and slightly varying data at HW. Thirdly, the model used only tidal boundary forcing. Thus, other meteorological effects (e.g. wind, waves and storms driven surges) might partially describe the difference between predicted and measured water levels.

In this analysis, we undertake long-term bed evolutions (15 years) applying the *MORFAC* technique. In this context, the present comparison of the hydrodynamic behavior provides sufficient confidence of our approach due to following reasons.

Table 2
Estimated Phase, Amplitude, Mean value and BSS of the predicted 1990 bed under three MORFAC approaches.

MORFAC	Phase	Amplitude	Mean value	BSS
30	0.075	0.129	0.093	-0.048
60	0.078	0.124	0.095	-0.041
120	0.081	0.124	0.100	-0.044

Table 3
Morphological simulations from 1975 to 1990 applying different bed sediment compositions.

Model No	Initial sediment characteristics			
	Name	Sediment fraction	Median grain size (d50, mm)	Distribution
M1	Single	sand	0.20	uniform
M2	Multiple	mud fine-sand coarse-sand	≤ 0.063 0.25 0.60	spatial

First, it is well known that a calibrated/validated model is quite likely to depart from the 'truth' the farther the simulation progresses past the calibration/validation period (Roelvink and Reniers, 2011). The deterministically chaotic nature of numerical models (Lorenz, 1972) is another phenomenon that places significant uncertainties on the quantitative accuracy of long term morphodynamic model predictions. Secondly, significant input reduction is required for long term simulations (i.e. present computational costs do not allow multiple long term brute force simulations). Therefore, even a model that is perfectly calibrated/validated (i.e. representing real forcing/response relationships), cannot be expected to predict future system response accurately due to the highly schematised nature of future forcing that is unavoidable in long term morphodynamic simulations. Finally, to develop a calibrated/validated model, it is required to have ample high quality calibration/validation data in 1975. This is clearly not the case as older hydrodynamic/morphology data is of questionable quality, and also very sparse (i.e. there are only monthly averaged water levels in the adjacent tidal basin and two measured bathymetries (1975 and 1990) of the study area during the applied morphological period).

4.1.2. Effect of Leyhörn on the Ley Bay hydrodynamic pattern

It is expected that maximum tidal flow in the basin/inlet systems occurs during the mid-tidal water levels (see Dissanayake et al., 2009). Therefore, the tidal flow pattern at mid-flood was analysed before (blue-vectors) and after (red-vectors) implementing Leyhörn to compare and contrast the effects (Fig. 9). These patterns suggest extensive tidal flats and salt marshes in the Ley Bay and provide first insight of the impact of Leyhörn on the existing flow pattern. At the west of the peninsula the tidal flow shows a weak velocity pattern after implementing the peninsula. This indicates that the peninsula interrupts the

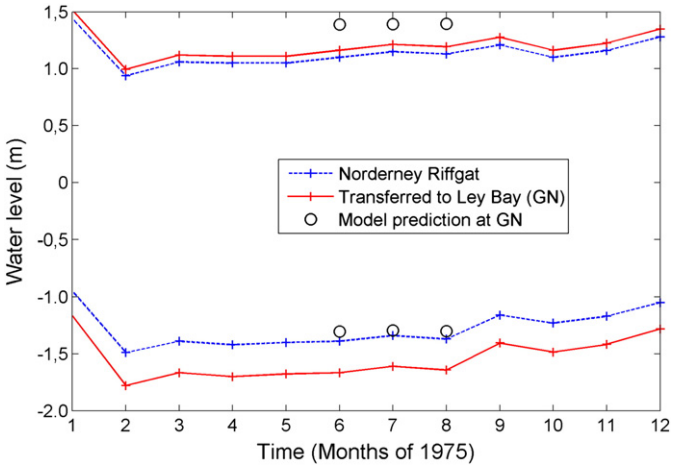

Fig. 8. Comparison of measured (transferred from Norderney Riffgat) and model predicted water levels at Greetsieler Nackenlegde (GN, see Figure a).

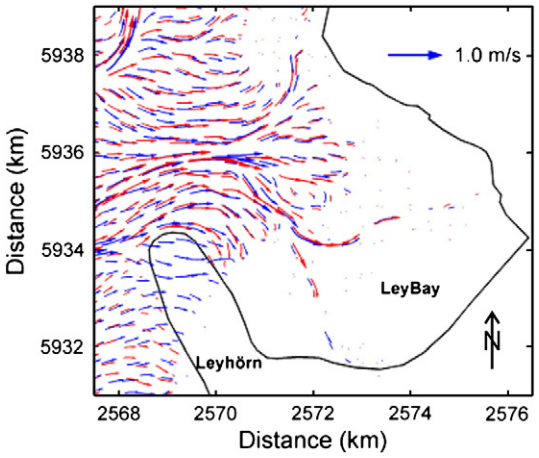

Fig. 9. Behaviour of tidal currents at mid-flood water level, before (blue) and after (red) implementing the effect of Leyhörn.

velocity vectors which are directed into the Ley Bay prior to the peninsula. At the north of the peninsula, the flow vectors are larger than the no-peninsula state implying that the peninsula results in strong bypassing of tidal currents due to the contraction of flow. In the Ley Bay area, the tidal currents tend to be eastward oriented and stronger with the peninsula than that of the no-peninsula state. This phenomenon is apparent by comparing the flow pattern in the channels (i.e. Leysander Priel, Greetsiler Watt. and Norder Außentief, see Fig. 3a for channel locations) under both situations.

According to the flow patterns, different sediment transport patterns can be expected also and consequently different erosion/sedimentation areas compared to the situation without the peninsula. Further, it is emphasised that the northeast directed sediment supply from the Ems estuary (on the west of the model area) into the Ley Bay area can be affected due to the construction of the peninsula.

4.2. Selection of mud-related parameters

To select the optimum values of mud-related parameters for the study area, a sensitivity analysis was undertaken of the most dominant five parameters on the sediment transport (e.g. Van der Wegen, 2010): 1) Shear stress for critical erosion ($\tau_{e,c}$), 2) Shear stress for critical deposition ($\tau_{d,c}$), 3) Dry bed density (ρ_{dry}), 4) Erosion parameter (M) and 5) Settling velocity (w). As discussed earlier, the sediment bed has a layered strategraphy of 10 layers of which the first layer consists of a transport layer and the first under layer. The transport layer thickness was set to 0.15 m following the analysis of Wehmeyer (2008) on the Eastern Wadden Sea area. Then, the first under layer thickness is 0.85 m. Three series of simulations were undertaken (i.e. applying the 1975 bathymetry for a 50 days period to investigate the relative effect on the bay sedimentation) and each series consists of five simulations of which only one parameter is modified in each model compared to the base case. Table 4 shows the applied mud-related parameters and their investigated values in 15 simulations and the base case simulation. Spatial distribution of $\tau_{e,c}$ is based on the fact that tidal flats consist of more consolidated material in comparison with the channel bed. Thus, the corresponding values for tidal flats and channels were applied as 0.48 and 0.14 respectively (Wehmeyer, 2008). The other values are based on previous research of the mud-transport (Van Ledden et al., 2004; 2006; Vander Wegen, 2010).

Table 4
Applied values of the sensitivity analysis for mud-related numerical parameters.

Model Parameter	Base model	Series 1	Series 2	Series 3
$\tau e,c$ (N/m2)	0.3	0.1	0.2	Spatial
$\tau d,c$ (N/m2)	100	0.2	10	50
ρdry (kg/m3)	380	500	600	800
M (kg/m2/s)	4.0×10^{-5}	3.8×10^{-5}	4.5×10^{-5}	6.0×10^{-5}
w (m/s)	4.7×10^{-4}	6.0×10^{-4}	8.0×10^{-4}	10.0×10^{-4}

Fig. 10 shows erosion and deposition volumes with respect to each series (refer number) and the model parameter together with the base case (refer black-dash line). It is emphasised that the volume estimation is based on the Ley Bay area only being our interested area (see enclosed rectangle in Fig. 3b). According to the selected value ranges, the highest sensitivity is found with the $\tau_{e,c}$ (critical erosion) while the w (settling velocity) shows the lowest sensitivity. Increasing $\tau_{e,c}$ implies lower erosion of the Oster-Ems basin and that results in lower deposition in the Ley Bay. Spatial application of $\tau_{e,c}$ shows higher deposition compared to *Series 2* and the base case due to having a lower $\tau_{e,c}$ in the channels (i.e. 0.14). Sediment deposition occurs when the bed shear stress is lower than $\tau_{d,c}$ (critical deposition). Thus, the higher the $\tau_{d,c}$ the higher the deposition. In contrary, the results indicate decreasing deposition as the $\tau_{d,c}$ increases. This is due to the strong sedimentation in the Oster-Ems basin and decrease sediment import into the Ley Bay. Similarly, higher ρ_{dry} (dry bed density) implies strong sedimentation outside the Ley Bay decreasing the sediment supply into the Ley Bay. Both erosion and deposition increase as the M (erosion parameter) increases. Deposition shows high sensitivity to the w compared to erosion (i.e. the higher the w the lower the deposition in the bay).

Data from 1975 to 1990 indicate strong sedimentation in the Ley Bay area (see Fig. 3). Therefore, the aforementioned model parameters were also tuned by selecting the value which resulted in the highest sedimentation in the bay (see values in bold-number in Table 4).

4.3. Morphodynamics

4.3.1. Visual comparison

Fig. 11 shows the predicted bed evolutions of M1 (single-sediment fraction) and M2 (multiple-sediment fraction) simulations in comparison to the measured data in 1975 and 1990. The Ley Bay area is characterised by a pattern of very shallow channels and shoals including a large area of tidal flats (see depth ranges). On the 1975 bed, the outline shows the proposed structure, Leyhörn (see Fig. 11a). On the 1990 bed, there is no navigational access channel through the peninsula because it has been implemented in 1991 (see Fig. 11b). From 1975 to 1990, data indicate strong sedimentation in the bay leading to disappear the basin channel pattern (see section 3.2.1 and Fig. 3a). However, the channel Leysander Priel appears to be more pronounced on the 1990 bed than on the 1975 bed. This indicates and eastward oriented velocity pattern at the entrance of the bay due to the effect of the peninsula as observed in Fig. 9.

Application of the single sediment fraction (M1) results in losing sediment from the bay (see shoal areas on Fig. 11c in comparison to Fig. 11a). Similar comparison indicates strong sedimentation by applying the multiple sediment fractions (see shoal areas on Fig. 11c in comparison to Fig. 11d). However, it is difficult to discern the difference of the basin channel pattern under both approaches and the data with respect to the bed evolution only.

Fig. 12 shows the erosion/sedimentation pattern from 1975 to 1990 in the data and the model predictions. Data clearly show strong sedimentation in the bay, along the channels and adjacent to the peninsula. These erosion/sedimentation areas comply with the observed velocity pattern (see Fig. 9). The channel, at the north end of the peninsula, shows strong sedimentation due to the impact of the peninsula under all cases. In case of the M1 simulation, bay channels appear to have deepened while a large part of the bay area remains unchanged indicating a sediment exporting system. Under the M2 simulation, the results show strong sedimentation (i.e. west of the peninsula; west and east of the bay in Fig. 12c). However, in some areas, they are not pronounced as found with the data (i.e. along the channels; north and east of the peninsula

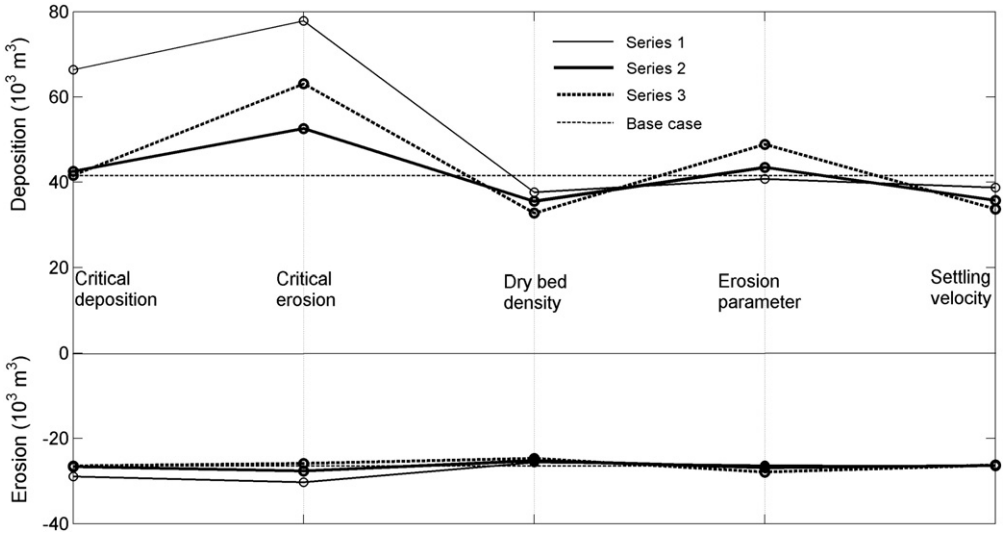

Fig. 10. Sensitivity of erosion and deposition to mud-related model parameters (in 50 days) in the Ley Bay with respect to Base case (black-dash line); Shear stress for critical deposition, Shear stress for critical erosion, Dry bed density, Erosion parameter and Settling velocity under three *Series* (refer number to Table 4).

in Fig. 12c). Therefore, the comparison indicates that the model prediction of the M2 partly reproduced the sediment distribution as found in the nature.

4.3.2. Statistical comparison

To quantitatively determine whether the single- or multiple-sediment fraction approach gives a better representation of the 1990 bathymetry, a statistical analysis was undertaken using the Brier Skill Score (*BSS*) (see section 3.2.4).

Fig. 13 shows the variation of the aforementioned parameters of the Ley Bay evolution (i.e. from 1975 to 1984 before implementing peninsula (solid-line) and from 1984 to 1990 after implementing the peninsula (dash-line)) based on the single (M1-blue) and multiple (M2-red) sediment fraction applications. The α (phase) of the M1 mildly increases starting from a lower value (Fig. 13a). In contrast, the M2 shows higher value even at the beginning (>0.15), which strongly increases after implementing the peninsula. Therefore, the bed level phases of the M2 are more in line with the data than the M1. In case of the M1, the β (amplitude) gradually increases during the morphological period while it decreases under the M2 (Fig. 13b). This also implies that the resulting bed level amplitudes of the M2 agree with the data rather than that of the M1. The γ (mean value) of the M1 remains more or less unchanged. However, it strongly decreases in the M2 leading to a higher agreement with the data (Fig. 13c). According to the behaviour of these three parameters, the bed form amplitude (β) dominates the *BSS* of the M1 while both amplitude and mean value (γ) affect the *BSS* of the M2. Only the evolution of the M2 model indicates increase of the *BSS* value after implementing the peninsula (Fig. 13d). Having higher *BSS* of the M2 suggests that the predicted evolution tends to agree with the data rather than the evolution under the M1. The predicted bed under the M2 can be defined as '*Good*' according to the classification of Sutherland et al. (2004) while it is '*Bad*' under the M1 (see Table 1).

4.3.3. Evolution of morphological elements

4.3.3.1. Basin hypsometry. Basin hypsometry describes the water surface area corresponding to the basin bed levels and thus represents the overall geometry of the basin. Fig. 14 shows the basin hypsometry in the Ley Bay area of the measured bathymetries (i.e. 1975 and 1990) in comparison to the model predictions (i.e. 1990 bed under M1 and M2 evolutions). Hypsometry of the 1990 data (dash-black-line) is located to the left of that of the 1975 data (solid-black-line). This implies decreased water surface area on the 1990 bed and in turn increased sedimentation in the basin. Both M1 (blue-line) and M2 (red-line) models resulted in different hypsometry curves indicating the effect of sediment characteristics on the evolution of the basin geometry. At deep areas (bed level <-4 m), the hypsometry of the M2 agrees with the data rather than the M1. This can probably be attributed to the pronounced Leysander Priel channel in the M2 compared to the M1 (compare Fig. 11c and d). The hypsometry of the M1 shows quite good agreement around MSL while the M2 indicates strong sedimentation. However, it is apparent that lower growth of shoal areas under this case (M1) tend to locate the hypsometry to the right of that of the data (see bed level $>$ MSL). Both M1 and M2 hypsometry curves agree at the top of tidal flat areas (see bed level $>$ MSL $+1$ m) which appear to have increased compared to the situation on the 1975

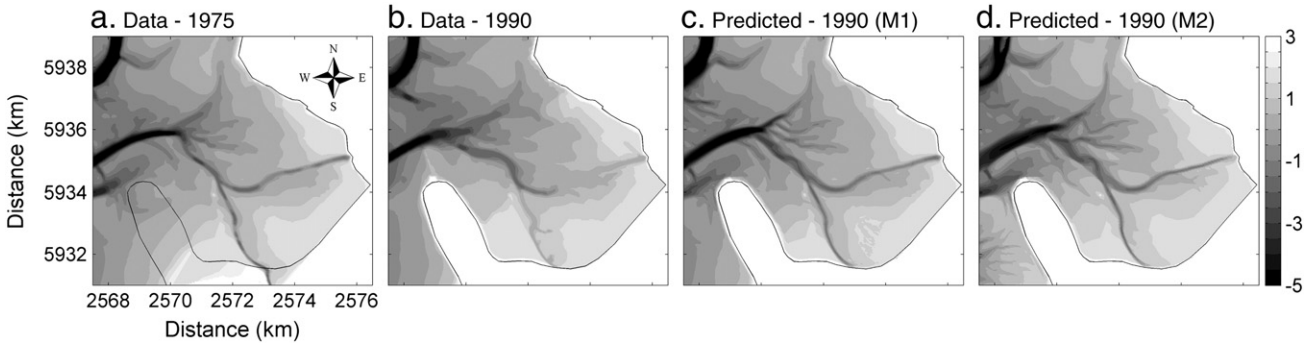

Fig. 11. Measured and model predicted bed evolutions in the Ley Bay area; Data-1975 (a), Data-1990 (b), Predicted-1990 (M1-single) (c) and Predicted-1990 (M2-multiple) (d).

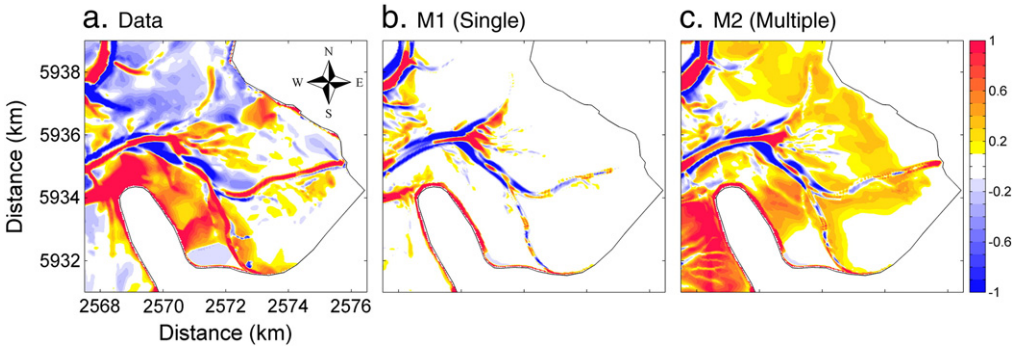

Fig. 12. Measured and model predicted erosion/sedimentation pattern from 1975 to 1990 in the Ley Bay area; Data (a), M1 (single) (b) and M2 (multiple) (c).

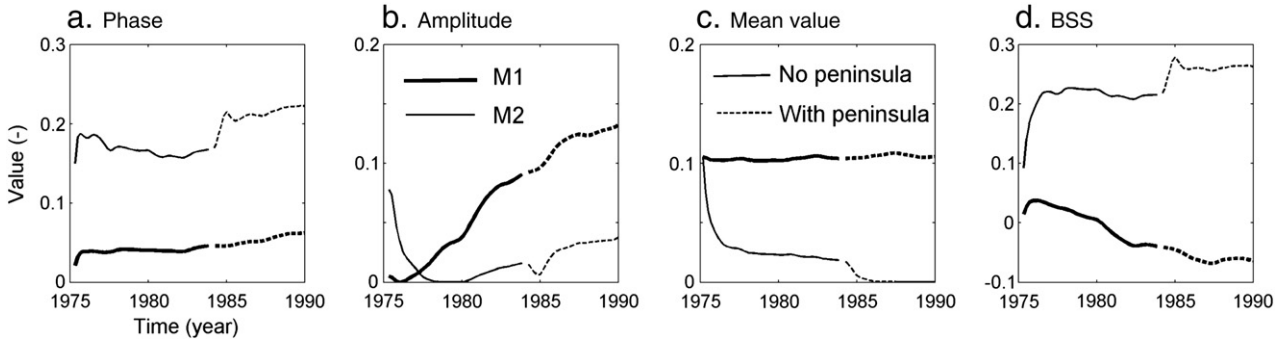

Fig. 13. Comparison of model results with the *BSS* of Sutherland et al. (2004); Phase (a), Amplitude (b), Mean value (c) and *BSS* (d) under M1 and M2 models.

measured bed. These hypsometry curves indicate strong sediment import into the Ley Bay under the case of M2 compared to that of the M1. However, the sediment distribution inside the bay of the M2 model weakly corresponds to that of the measured data (see around MSL).

The hypsometry showed the basin geometry of the final predicted bed (i.e. model prediction in 1990). Further analysis is undertaken to investigate the temporal evolution of the basin geometry in terms of the channel and tidal flat evolutions.

4.3.4. Channels and tidal flats in the Ley Bay

Channel volume is the water volume in the bay below mean low water (MLW) and the wet area at MLW is defined as the channel area (see V_c and A_c in Fig. 15). Volume of tidal flats is the shoal volume that exists between MLW and mean high water (MHW) levels in the bay and the corresponding dry area is estimated as the tidal flat area (see V_f and A_f in Fig. 15). Accordingly, the channel parameters are based on MLW only while the tidal flat parameters depend on the tidal range.

Fig. 16 shows the evolution of channel and tidal flat parameters of the data and the model predictions. The Ley Bay area is characterised by a small channel system and extensive tidal flat areas as described in section 2.0. This is evident in Fig. 16 also by comparing *y*-axis of flat area and channel area, flat volume and channel volume. Predicted evolutions show crests and troughs in each parameter. These features in morphological time scale correspond to spring- and neap-tide

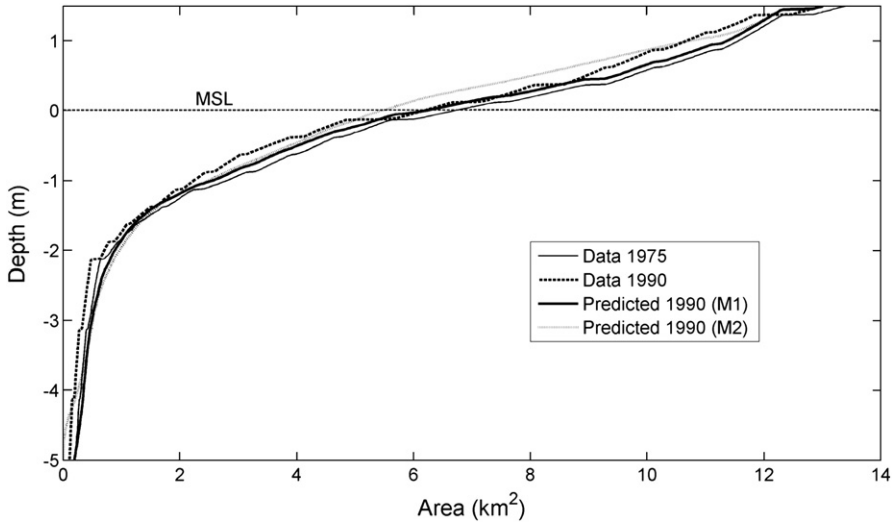

Fig. 14. Basin hypsometry of the Ley Bay area of the measured beds; 1975 (solid-thin-line) and 1990 (dash-thick-line) and model predictions; M1 (solid-thick-line) and M2 (dotted-line).

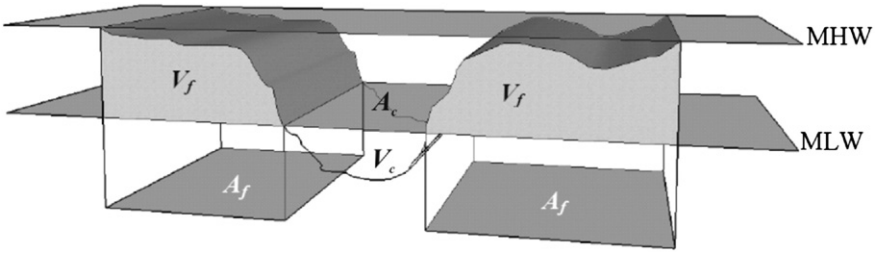

Fig. 15. Definition of channel volume (V_c), channel area (A_c), tidal flat volume (V_f) and tidal flat area (A_f).

respectively in case of the tidal flat evolution and vice versa of the channel evolution during the hydrodynamic period of three months. Predicted results at 1975 are slightly different to the data. This is expected due to analysing the results after excluding the initial period which was applied to stabilise the model. Evolution of these parameters after 1984 shows the effect of the Leyhörn peninsula (i.e. solid-line without peninsula and dash-line with peninsula).

Both M1 and M2 models predict more or less similar evolution of the tidal flat area (Fig. 16a). However, the results of the M2 show lower flat areas at troughs. This is an indication of different channel bank slopes of the predicted beds during neap-tide (see Friedrichs et al., 1990). After implementing the peninsula (dash-line), both models predict lower areas compared to the situation without the peninsula (solid-line). This is mainly due to excluding the area enclosed by the peninsula which consists of shoal areas (see Fig. 11a). Both approaches resulted in almost similar flat area on the 1990 bed and that slightly overestimates the data. Evolution under the M2 model resulted in the highest tidal flat volume (Fig. 16b). Similar behaviour is found after implementing the peninsula also. In this case, the contrasting pattern of lower flat area (i.e. after implementing the peninsula) and higher flat volume is related to the fact that the area considers the aerial extent while the sediment amount is estimated as the volume. Resulting flat volume under the M1 is lower compared to that of the M2 and it appears to resemble with the 1990 data.

At neap-tide, channel area is higher and it is similar under both modelling approaches (see crests in Fig. 16c). This is due to the highest MLW at this condition. Further, after implementing the peninsula, the channel area decreases in both cases. This is again due to excluding the area of the peninsula. The channel area also depends on the geometry as discussed in Friedrichs et al. (1990). Predicted channel area on the 1990 bed under the M1 appears to correspond with the data than that of the M2. In case of the channel volume, the M2 model predicts lower channel volume which further decreases after implementing the peninsula (Fig. 16d). This indicates lower water volume in the bay under MLW and in turn higher sediment import. In this case, the predicted channel volume on the 1990 bed agrees with that of the 1990 data. On the 1990 bed, in contrast to the evolution of channel area, the M1 model predicts higher channel volume (i.e. ~ 0.5 Mm^3 higher than the data). This also appends to the definition of area and volume.

Analysis on the tidal flat and channel evolutions provided an overall estimation of the channel/shoal pattern in the bay. However, these did not provide an insight on the bed configurations (i.e. slope of the channel banks, width and depth of the channels, extent of shoals etc.) under the

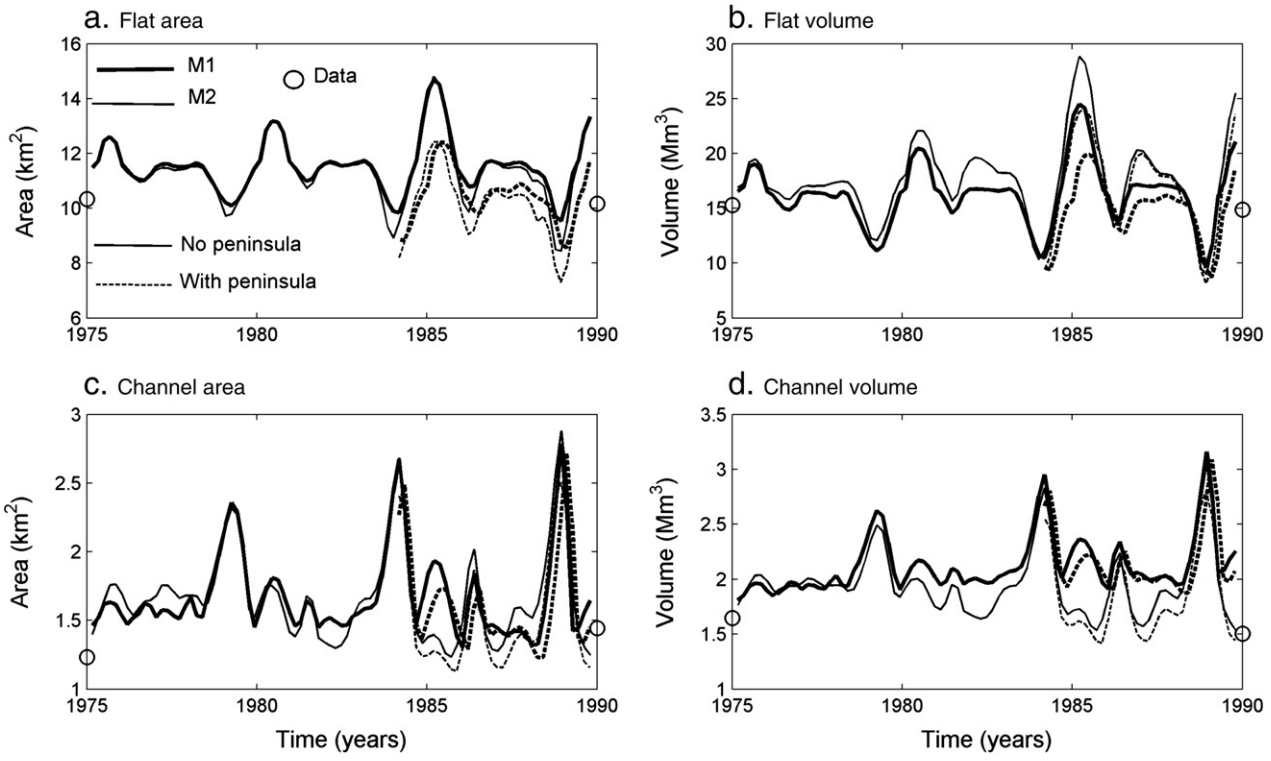

Fig. 16. Evolution of basin parameters from 1975 to 1990 in Data (○), M1 (solid-thick-line) and M2 (solid-thin-line) models; flat area (a), flat volume (b), channel area (c) and channel volume (d). Note: solid line without peninsula and dash line with peninsula.

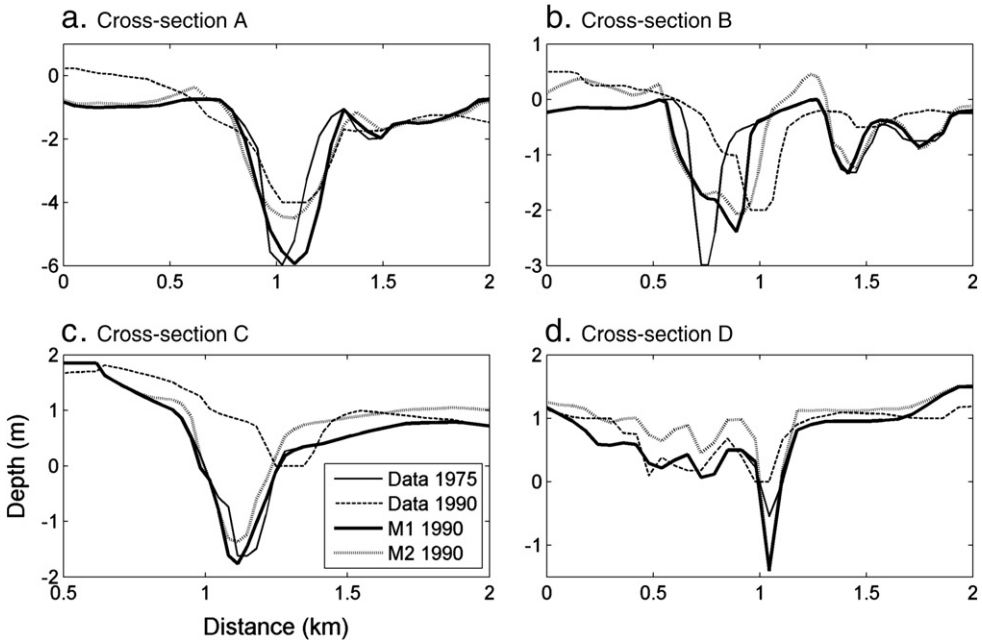

Fig. 17. Predicted channel evolutions; M1 (solid-thick-line), M2 (dotted-line) with the measured data; 1975 (solid-thin-line), 1990 (dash-thin-line) at Cross-section A (a), B (b), C (c) and D (d).

model predictions and data. Therefore, a few cross-sectional evolutions are compared to investigate the latter aspects.

4.3.5. Cross-sectional evolution of basin channels

Evolution of a few channel cross-sections (i.e. A, B, C and D, see Fig. 1) was undertaken to further compare and contrast the model predictions with the data. Cross-section A is in the main channel Norderley (maximum depth ~ 6 m) and it is located just outside of the bay. Cross-section B is in the bay entrance channel Leysander Priel (maximum depth ~ 3 m). The other two cross-sections are located at the distal parts of the bay channels, Greetsieler Wattfahrwasser (C, maximum depth ~ 1.5 m) and Norder Außentief (D, maximum depth ~ 0.5 m). These cross-sectional depths strongly decrease from A to D.

Fig. 17 shows the cross-sectional evolution of the model predictions in comparison to the data in 1975 and 1990. At the cross-section A, the M1 model predicts widening while maintaining the initial depth. The M2 model tends to reproduce the channel as present in the data. Both model results agree with the shoal areas on the right and underestimate the shoal areas on the left (i.e. adjacent to the peninsula). At the cross-section B, both models predict evolution towards the data. The shoal area on the left agrees with the data under the M2 model. Therefore, the M2 model generally shows good agreement with the data compared to the M1 model. At the cross-section C, the evolution of both models weakly resembles the data. However, the predicted cross-section under the M2 appears to resemble with data in respect of the shoal areas on the right. In this case also, data indicate rightward orientation of the cross-sectional growth. Evolution of the cross-section D shows contrasting behaviour in comparison to the other sections. Depth of the predicted sections increases while data indicate decreasing. The shoal areas on the right agree with the data under both models though it appears to have been overestimated on the left under the M2 model.

Further analysis of these cross-sectional evolutions was undertaken considering, 1) Maximum depth (m), 2) Lateral displacement (m) and 3) Area (10^3 m^2). Maximum depth indicates the deepest point of the cross-sectional profile. Lateral displacement was estimated with respect to the 1975 bed and the rightward displacements are given in positive values. Cross-sectional area was computed below mean sea level (MSL). For example, if the cross-section is located above MSL, corresponding area is zero.

Table 5 shows the estimated values of these parameters. As discussed earlier, strong sedimentation of the Ley Bay area is evident by comparing the maximum depth and area of the cross-sections on the 1975 and 1990 beds. Estimated values of the M2 model show relatively high agreement with the data rather than that of the M1 model. Both models have reproduced the lateral displacement at cross-section A while the major difference between the data and the model predictions is obtained at cross-sections B and C. This indicates that additional processes which are not applied in the models, govern the morphology around the cross-sections B and C. A likely explanation is found in the dredging and dumping work from 1975 to 1990 (see section 3.2.5) which may have resulted in the rightward displacement of these two sections.

The predicted bed evolutions show some deviations from the measured data. These are likely related to the omission of wave boundary forcing, dredging/dumping activities and to schematised sediment characteristics. Only the effect of the sediment characteristics is further investigated in this study by applying different initial sediment distributions. On-going study focuses on the impact of dredging/dumping activities and wave effects on the Ley Bay evolution.

Table 5
Maximum depth, Lateral displacement and Area of the cross-sections A, B, C and D (see Figure) on measured data (1975 and 1990) and model predictions (M1 and M2).

Parameter	Maximum depth (m)				Lateral displacement (m)			Area (10^3 m^2)			
Cross-section	1975	1990	M1	M2	1990	M1	M2	1975	1990	M1	M2
A	-5.9	-4.0	-5.9	-4.2	58	58	58	3.33	2.94	3.67	3.35
B	-2.9	-2.0	-2.3	-2.1	234	132	166	0.99	0.78	1.21	1.14
C	-1.6	0	-1.7	-1.4	166	-16	-16	0.24	0	0.25	0.19
D	-0.5	0	-1.4	-1.4	-33	0	0	0.03	0	0.08	0.07

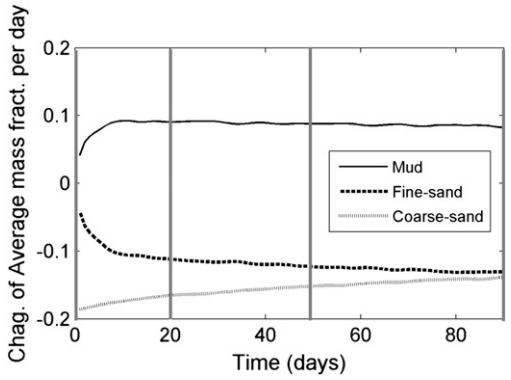

Fig. 18. Evolution of averaged mass fraction per day; Mud (solid-line), Fine-sand (dash-line) and Coarse-sand (dotted-line). Vertical lines (t = 0, 20, 50 and 90) indicate selected sediment maps for the morphological runs.

4.3.6. Applying initially distributed sediment fractions

Initially distributed sediment maps were developed by simulating the M2 model to allocate the sediment distribution without bed level changing (see Van der Wegen, 2010). Sediment distribution of the top layer was used as an indication to estimate whether it has reached a stable state. The averaged mass fraction per day of each sediment fraction at the top layer was computed in the Ley Bay area (Fig. 18). Initially, all sediment fractions show strong evolution; this tends to decrease as the grain size increases. Thus, the lower the grain size the faster the sediment composition reaches a stable condition. Such phenomenon is expected due to the highest mobility of the smallest particles (i.e. mud fraction).

Fig. 19 shows the distribution of sediment fractions at the top layer for three model predicted sediment maps (t = 20, 50 and 90 days in Fig. 18). As the time increases, the mud fraction has concentrated towards the borders of the bay and the distal parts of the channels. In the mean time, the fine sand fraction has escaped from the channel bed and the presence of the coarse sand fraction in the channels has increased.

Resulting bed evolutions from 1975 to 1990 applying these three sediment maps (Fig. 19) were compared with that of the M2 model and the measured data.

For the reason clarity, analysis of the cross-sectional evolutions is limited to t = 0, 20 and 50 cases and the data in 1975 and 1990 (Fig. 20). At the cross-section A, application of t = 0 and 20 sediment maps shows comparable evolution as in the data while t = 50 case implies the highest difference. Similar observation is apparent at the cross-section B also though the t = 20 case indicates slightly lower sediment import into the bay than that of t = 0. At the cross-section C, the predicted evolution in all cases is similar to that of the 1975 data indicating that the models have underestimated sediment supply into this area. Application of the initially distributed sediment fractions shows a significant improvement at the cross-section D (Fig. 20d). As discussed earlier, the M2 model (t = 0) resulted in deepening this area rather than the initial state (i.e. 1975 bed). In contrast, the models applying the initially distributed sediment fractions predict that this channel section remains unchanged (i.e. similar to 1975 bed) and the surrounding shoal areas better agree with the 1990 data. Accordingly, the cross-sectional evolutions suggest the optimal bed evolution in the Ley Bay under the t = 20 case. Therefore, application of the initially distributed sediment fractions (at t = 20) is able to sufficiently reproduce the effect of the Leyhörn peninsula

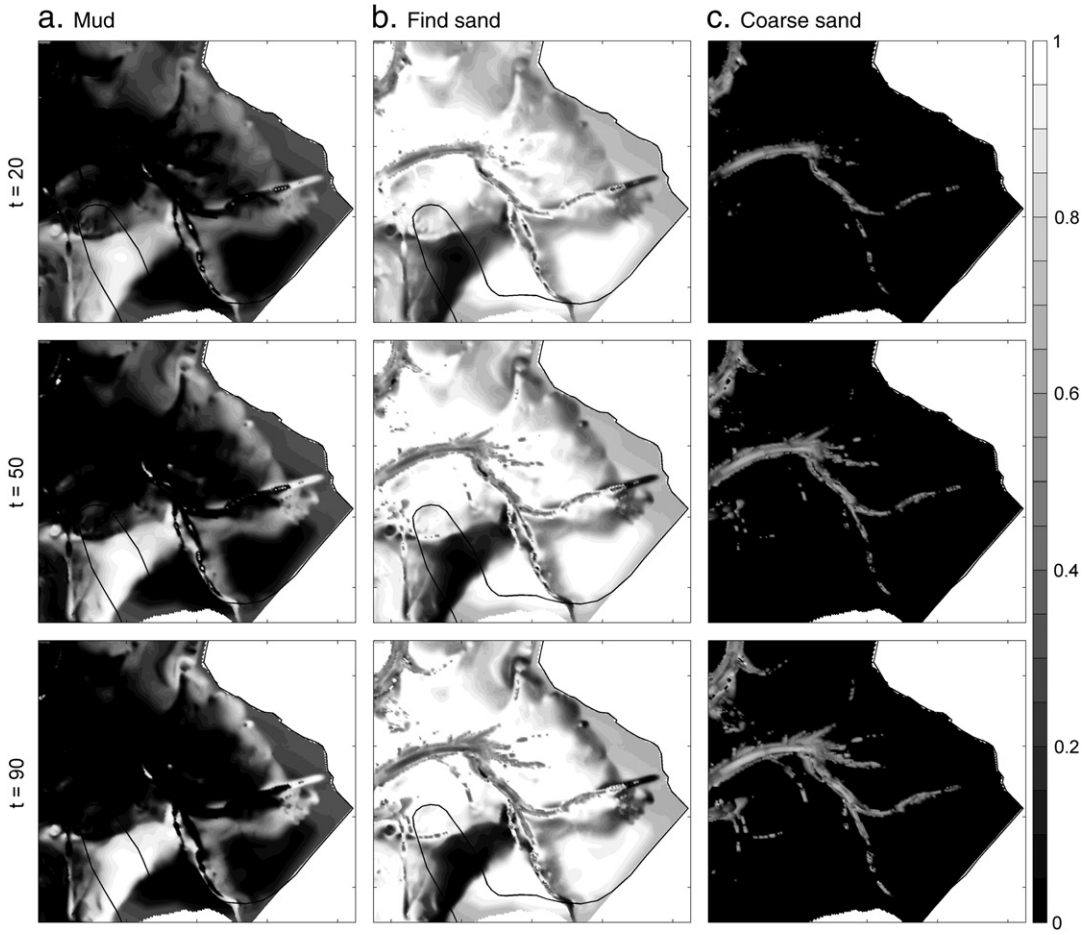

Fig. 19. Distribution of sediment fractions at the top layer; a) Mud, b) Fine-sand and c) Coarse-sand at t = 20, 50 and 90 days of initially distributed sediment maps from Figure.

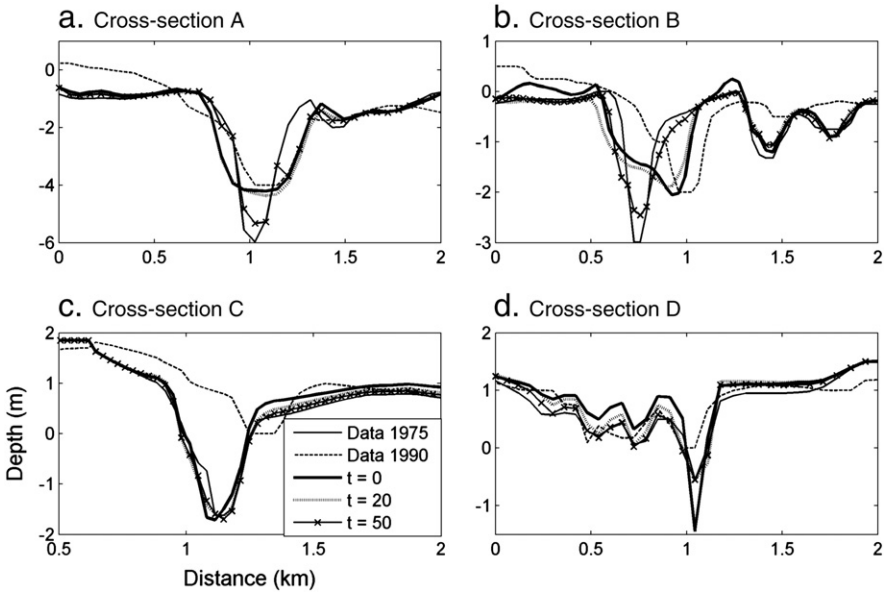

Fig. 20. Cross-sectional evolution with data; 1975 bed (solid-thin-line), 1990 bed (dash-thin-line) and model predictions; M2 (initial sediment map at t = 0 from Figure , solid-thick-line), applying initially distributed sediment maps (t = 20, dotted-line and t = 50, solid-cross-line from Figure).

on the Ley Bay morphology in comparison to the other bed sediment compositions.

5. Conclusions

Potential physical impacts of an anthropogenic effect on a tidal basin evolution are investigated using the state-of-the-art Delft3D numerical model. Study area is based on the Ley Bay in the East Frisian Wadden Sea. The model simulations span 15 years (from 1975 to 1990) and are only driven by tidal boundary forcings, while using different bed sediment compositions, viz. a single sediment fraction (M1: $d_{50} = 0.2$ mm) and multiple sediment fractions (M2: mud (≤ 0.063), fine-sand (0.25) and coarse-sand (0.60)). Additional simulations were undertaken applying an initially distributed sediment content which is derived based on the multiple fractions.

Predicted water levels in the Ley Bay area showed reasonable agreement with the monthly averaged data in 1975 (i.e. agreement at HW is higher than LW). It is generally accepted that the models have difficulties representing LW in the Wadden Sea area due to the extensive tidal flats. Simulated hydrodynamic patterns on the 1975 and 1990 beds showed the impact of the Leyhörn viz. strong contraction of velocities at the Ley Bay entrance, strong velocities along the easterly directed basin channel (i.e. Norder Außentief), and weak velocities at the west of the peninsula. The optimal values of the cohesive-sediment parameters were selected to obtain strong sedimentation in the Ley Bay as found with the data. Sedimentation and erosion patterns indicate the highest sediment import into the Ley Bay area under the M2 model. The predicted evolution after 15 years of this model can be classified as '*Good*' according to the *BSS* criterion of Sutherland et al. (2004). Evolution of the basin elements (i.e. channels and tidal flats) of the M2 model showed better agreement with the data rather than M1. These evolutions indicate the effect of the peninsula; strong reduction of basin elements immediately after implementing the peninsula, later strong growth of tidal flats and decreased channels due to increased sediment import. Cross-sectional evolutions further showed increased sediment import into the bay and a better agreement with the data in the case of the M2. Under the application of initially distributed sediment fractions, a significant improvement of the predicted evolution was observed at the shallowest cross-section in comparison to the M2 simulation. These results suggest that applying an initially distributed sediment content, which is stable with the boundary conditions, largely reproduces the peninsula effect on the Ley Bay morphology.

Resulting evolutions indicate that it is necessary to include other effects such as wave input and dredging/dumping activities. Ongoing study investigates these aspects and that will be discussed in a separate manuscript.

Acknowledgements

The work presented in this paper was carried out under the project of 'Veränderliches Küstenklima - Evaluierung von Anpassungsstrategien im Küstenschutz (A-KÜST: Changing Coastal Climate – Evaluation of Adaption Strategies for Coastal Protection)' as a part of 'Klimafolgenforschung Szenarien für die Klimaanpassung' (KLIFF: Climate Impact Research for Adaption)' funded by the Lower Saxon State Ministry for Science and Culture, Germany.

References

Dastgheib, A., Roelvink, J.A., Wang, Z.B., 2008. Long-term process-based morphological modelling of the Marsdiep Tidal Basin. Marine Geology 256, 90–100.
Dissanayake, D.M.P.K., Roelvink, J.A., Van der Wegen, M., 2009. Modelled channel pattern in schematised tidal inlet. Coastal Engineering 56, 1069–1083.
Dissanayake, D.M.P.K., Ranasinghe, R., Roelvink, J.A., 2012. The morphological response of large tidal inlet/basin systems to Relative Sea level rise. Climatic Change, http://dx.doi.org/10.1007/s 10584-012-0402-z.
Elias, E., 2006. Morphodynamics of Texel Inlet, IOS Pres, PhD Thesis, Technical University of Delft, ISBN 1-58603-676-9.
Elias, E., Stive, M.J.F., Bonekamp, J.G., Cleveringa, J., 2003. Tidal inlet dynamics in response to human intervention. Coastal Engineering 45 (4), 629–658.
Friedrichs, C.T., Aubrey, D.G., Speer, P.E., 1990. Impacts of Relative Sea-level Rise on Evolution of Shallow Estuaries, Coastal and Estuarine Studies, Vol. 38. In: Cheng, R.T. (Ed.), Residual Currents and Long-term Transport. Springer-Verlag, New York.
Galappatti, R., 1983. A depth integrated model for suspended transport, Report 83–7. Department of Civil Engineering, Delft University of Technology, Communications on Hydraulics.
Hartsuiker, G., 2003. Tidal Model Weser Estuary, Set-up and calibration of flow model, Report Alkyon, pp. 15–17.
Hartung, W., 1983. Die Leybucht (Ostfriesland) – Probleme ihrer Erhalttung als Naturschutzgebiet, Neues Archiv f. Niedersachsen, Bd. 32, H. 4, Göttingen, pp. 355–387.
Hayes, M.O., 1979. Barrier island morphology as a function of tidal and wave regime, in proceeding of the coastal symposium of barrier islands. edited by S.P. Leatherman, Academic press, New York. 1–28.
Herrling, G., Niemeyer, H.D., 2008. Set-up of a morphodynamic model for the Ems-Dollard estuary, HARBASINS report, pp. 9–10.
Homeier, H., 1969. In: OHLING, H. (Ed.), Der Gestaltenwandel der Ostfriesischen Küste im Laufe der Jahrhunderte – Ein Jahrtausend ostfriesischer Deichgeschichte: Ostfriesland im Schutz des Deiches, 2, pp. 3–75. Deichacht Krummhörn, Pewsum.

Homeier, H., Stephan, H.J., Niemeyer, H.D., 2010. Historisches Kartenwerk Niedersächsische Küste der Forschungsstelle Küste. Niedersächsischer Landesbetrieb für Wasserwirtschaft Küsten- und Naturschutz (NLWKN)Geschäftsbereich Gewässerbewirtschaftung und Flussgebietsmanagement.
Knaack, H., Niemeyer, H.D., 2001. Morphodynamische Gleichgewichtszustände in der Leybucht zwischen 1960 und 1999, Dienstbericht. Niedersächsisches Landesamt für Ökologie, Forschungsstelle Küste, Norderney. (in Deutsch).
Knaack, H., Kaiser, R., Niemeyer, H.D., 2003. Mathematische Modellierung von Tiden in der Leybucht, Dienstbericht. Niedersächsisches Landesamt für Ökologie, Forschungsstelle Küste, Norderney. (in Deutsch).
Leendertse, J.J., 1987. A three-dimensional alternating direction implicit model with iterative fourth order dissipative non-linear advection terms. WD-333-NETH. Rijkswaterstaat, The Netherands.
Lesser, G.R., Roelvink, J.A., Van Kester, J.A.T.M., Stelling, G.S., 2004. Development and validation of a three-dimensional morphological model. Coastal Engineering 51, 883–915.
Lorenz, E.N., 1972. Predictability: Does the flap of a butterfly's wings in Brazil set off a tornado in Texas? American Asso. for the Advancement of Science Annual Meeting Prog, p. 139.
Niemeyer, H.D., 1984. Hydrographische Untersuchungen in der Leybucht zum Bauvorhaben Leyhörn. Jahresbericht 1983 Forschungsstelle f. Insel- u. Küstenschutz, Bd. 35, Norderney, pp. 61–98.
Niemeyer, H.D., 1991. Case study Ley Bay, an alternative to traditional enclosure. Proc. 3rd Conf. on Coastal and Port Engineering in Developing Countries (COPEDEC), Mumbasa, Kenya.
Niemeyer, H.D., 1994. Hydrodynamical Investigations for Coastal Protections Measures, Case Study Ley Bay. Proc. Int. Conf. Hydrodyn. '94, Wuxi, China.
Niemeyer, H.D., Kaiser, R., Brandt, G., Glaser, D., 2001. Beweissicherung Küstenschutz Leybucht-Überprüfung der Tnw-Abschätzung für das Leysiel. Dienstbericht 5/2001, Niedersächsisches Landesamt für Ökologie-Forschungsstelle Küste, Norderney. (unveröffentlicht).
Partheniades, E., 1965. Erosion and Deposition of Cohesive Soils. Journal of the Hydraulic Division, ASCE 91 No. HY1.
Pedrozo-Acuna, A., Simmonds, D.J., Otta, A.K., Chadwick, A.J., 2006. On the cross-shore profile change of gravel beaches. Coastal Engineering 53, 335–347.
Ridderinkhof, H., 1988. Tidal and residual flows in the Western Dutch Wadden Sea 1: Numerical model results. Netherlands Journal of Sea Reasearch 22 (1), 1–21.
Rijkswaterstaat Sediment Atlas, 2007. Rijkswaterstaat Waterdienst, Lelystad. http://www.waddenloket.nl/index.php?id=729.
Roelvink, J.A., 2006. Coastal morphodynamic evolution techniques. Coastal Engineering 53, 277–287.
Roelvink, J.A., Reniers, A.J.H.M., 2011. A guide to modelling coastal morphology. Advances in Coastal and Ocean Engineering. World Scientific.
Roelvink, D., Reniers, A., Van Dongeren, A., De Vries, J.V.T., McCall, R., Lescinski, J., 2009. Modelling storm impacts on beaches, dunes and barrier islands. Coastal Engineering 56, 1133–1156.
Ruessink, B.G., Walstra, D.J.R., Southgate, H.N., 2003. Calibration and verification of a parametric wave model on barred beaches. Coastal Engineering 48, 139–149.
Ruggiero, P., Walstra, D.J.R., Gelfenbaum, G., Van Ormondt, M., 2009. Seasonal-scale nearshore morphological evolution: Field observations and numerical modelling. Coastal Engineering 56, 1153–1172.
Sha, L.P., 1989. Variation in ebb-delta morphologies along the West and East Frisian Islands. The Netherlands and Germany, Marine Geology 89, 11–28.
Stelling, G.S., 1984. On the construction of computational methods for shallow water flow problem. Rijkswaterstaat Communications vol. 35. Governing printing Office, The Hague, The Netherlands.
Stelling, G.S., Leendertse, J.J., 1991. Approximation of convective processes by cyclic AOI methods. Proceeding of the 2nd ASCE Conference on Estuarine and Coastal Modelling, Tampa. ASCE, New York, pp. 771–782.
Stive, M.J.F., Roelvink, J.A., De Vriend, H.J., 1990. Large-scale coastal evolution concept. Proc. 22nd Int. Conf. on Coastal Engineering. ASCE, New York.
Sutherland, J., Peet, A.H., Soulsby, R.L., 2004. Evaluating the performance of morphological models. Costal Engineering 51, 917–939.
Thijsse, J.T., 1972. Een halve Zuider Zeewerken 1920–1970. Tjeenk Willink, Groningen.
Van der Wegen, M., 2010. Modelling morphodynamic evolution in alluvial estuaries, PhD Thesis. UNESCO-IHE Institute for Water Education.
Van der Wegen, M., Roelvink, J.A., 2008. Long-term morphodynamic evolution of a tidal embayment using a two-dimensional process-based model. Journal of Geophysical Research 113, C03016, http://dx.doi.org/10.1029/2006JC003983.
Van der Wegen, M., Roelvink, J.A., De Ronde, J., Van der Speck, A., 2008. Long-term morphodynamic evolution of the Western Scheldt estuary, The Netherlands, using a process-based model. COPEDEC VII, Dubai, UAE.
Van Ledden, M., Wang, Z.B., Winterwerp, H., De Vriend, H., 2004. Sand-mud morphodynamics in a short tidal basin. Ocean Dynamics 54, 385–391.
Van Ledden, M., Wang, Z.B., Winterwerp, H., De Vriend, H., 2006. Modelling sand-mud morphodynamics in the Friesche Zeegat. Ocean Dynamics 56, 248–265.
Van Rijn, L.C., 1993. Principles of sediment transport in rivers, estuaries and coastal seas. AQUA Publications, the Netherlands.
Verboom, G.K., De Ronde, J.G., Van Dijk, R.P., 1992. A Fine Grid Tidal Flow and Storm Surge Model of the North Sea. Continent. Shelf Research 12.
Wang, Z.B., Louters, T., De Vriend, H.J., 1995. Morphodynamic modelling for a tidal inlet in the Wadden Sea. Marine Geology 126, 289–300.
Wehmeyer, C., 2008. Sensitivity Analysis and Calibration of a Morphodynamic Model for Pit Backfill, M.Sc. thesis, Christian Albrechts University, Kiel, Germany.